Fabrication of 2D Block Copolymer Brushes via a Polymer-Single-Crystal-Assisted-Grafting-to Method

Shan Mei,[1] Jeffrey T. Wilk,[1] Andrew J. Chancellor,[2] Bin Zhao,[2,] and Christopher Y. Li[1,*]*

[1]Dr. Shan Mei, Jeffrey T. Wilk, Prof. Christopher Li, Department of Materials Science and Engineering, Drexel University, Philadelphia, Pennsylvania 19104, United States

[2]Andrew J. Chancellor, Prof. Bin Zhao, Department of Chemistry, University of Tennessee, Knoxville, Tennessee 37996, United States

* Correspondence to: chrisli@drexel.edu; bzhao@utk.edu

Abstract

Block copolymer brushes are of great interest due to their rich phase behavior and value-added properties compared to homopolymer brushes. Traditional synthesis involves grafting-to and grafting-from methods. In this work, a recently developed "polymer-single-crystal-assisted-grafting-to" method is applied for the preparation of block copolymer brushes on flat glass surfaces. Triblock copolymer poly(ethylene oxide)-*b*-poly(L-lactide)-*b*-poly(3-(triethoxysilyl)propyl methacrylate) (PEO-*b*-PLLA-*b*-PTESPMA) was synthesized with PLLA as the brush morphology-directing component and PTESPMA as the anchoring block. PEO-*b*-PLLA block copolymer brushes are obtained by chemical grafting of the triblock copolymer single crystals onto a glass surface. The tethering point and overall brush pattern are determined by the single crystal morphology. The grafting density is calculated to be ~ 0.36 nm^{-2} from the atomic force microscopy

results and is consistent with the theoretic calculation based on the PLLA crystalline lattice. This work provides a new strategy to synthesize well-defined block copolymer brushes.

Keywords: polymer brushes • block copolymer brushes • polymer single crystal • polymer crystallization

Polymer brushes are thin layers of polymers tethered on substrates.[1] They are of great scientific interest and have also been widely used to modify solid flat and curved surfaces.[1] Recent developments in synthetic techniques combined with new theories have established a platform for the emergence of polymer brushes with various structures as well as new applications.[2] Among these, block copolymer brushes are of particular interest due to the rich phase behavior and potential applications associated with their binary chemical structures[3]. For example, both theoretical and experimental studies have revealed the complex phase behavior of block copolymer brushes, which is related to chain length, chain symmetry, χ value, grafting density, etc.[4] Block copolymer brushes can be used for stimuli-responsive surface[5], controlled release[6], anti-fouling[7], modulated gating[8], self-assembly[9], cell attachment control,[10] and emulsion stabilization[11], etc. Traditional synthesis includes grafting-to and grafting-from methods, where grafting-from is more frequently used due to the high brush molecular weight and high grafting density that it can offer. Tremendous efforts have been devoted to the development of synthetic methods, especially surface-initiated controlled radical polymerizations, which have a relatively good control over molecular weight and dispersity. Block copolymer brushes can be prepared by

careful sequential surface-initiated "living"/controlled polymerization, such as atom transfer radical polymerization (SI-ATRP) or reversible addition-fragmentation chain transfer polymerization (SI-RAFT), when different monomers are used.[12]

Polymer single crystals (PSCs) have been studied for decades and recent studies show that they can be used as a powerful tool to fabricate nanostructured materials.[13] For example, polymer crystallization has been employed to guide block copolymer assembly into precisely controlled structures, such as 1D micelles, disks, and crystalsomes.[14] Polymer single crystals have also been used for hairy nanoparticle synthesis and assembly,[15] directing ion transport,[16] and fabricating long-circulating block copolymer crystalsomes,[17] etc. Recently, a novel "polymer-single-crystal-assisted-grafting to"(PSCAGT) method has been developed for the synthesis of polymer brushes with controlled grafting density and tethering points.[18] In this method, end-functionalized polymers crystallize into 2D PSCs followed by coupling to surfaces (**Figure 1a**). Integral chain folding enables the exposure of functional chain ends on the PSC surfaces, which can be coupled onto a solid surface (e.g., glass) to serve as the tethering points of polymer brushes. Previous work has been focused on the preparation of homopolymer single-stranded, looped, and patterned brushes. While block copolymer single crystals are used as a model system to study brush behavior, they are free-standing crystals.[19] When adapting this method to synthesize block copolymer brushes, simply using an end-functionalized diblock copolymer does not yield the desired structure because the end-functional groups can be easily shielded by amorphous chains, leading to low coupling efficiency and low grafting density (**Figure 1b**). Herein, we report the synthesis of diblock copolymer brushes using a semicrystalline triblock copolymer as the template, as shown in **Figure 1c**. The three blocks have distinct functions in the brush synthesis, namely single-crystal-templating and brush-forming (blue), tethering (red), and brush-forming (green). Using this

approach, highly efficient coupling can be achieved and the resultant diblock copolymer brushes showed a relatively high grafting density of 0.36 ± 0.1 nm^{-2}. The brushes formed using this method also retain original single crystal morphology with high fidelity, providing a unique means towards patterned polymer brushes.[18b]

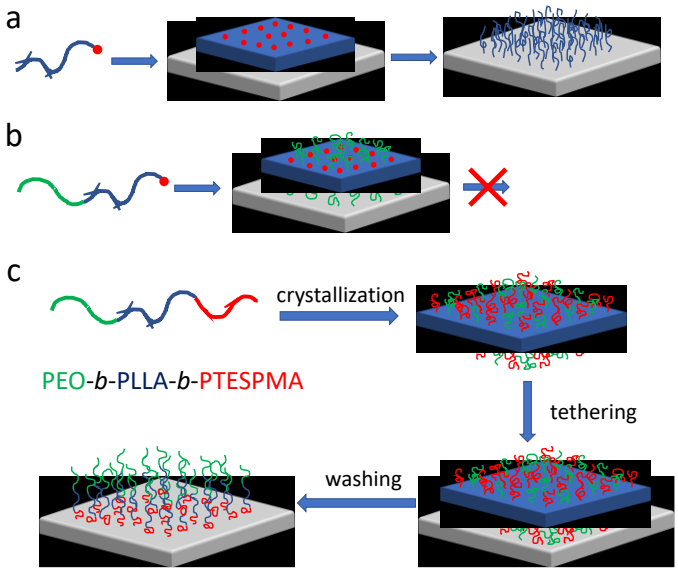

Figure 1. Schematics of polymer brush synthesis through the PSCAGT method. a) Homopolymer brushes are formed by utilizing end-functionalized homopolymer single crystals as the template. The red dot at the end of the chain represents a functional coupling group. B) Diblock copolymer with an end-functional group (red dot) cannot form diblock brushes using the PSCAGT method due to the shielding effect of the uncrystallized chains (red) in the block copolymer single crystals. c) Triblock copolymer with crystalline (blue) and coupling (red) blocks can be used to form diblock copolymer brushes. Single crystals of the triblock copolymer can be chemically coupled to the surface. Subsequent removal of untethered chains leads to PEO-*b*-PLLA diblock copolymer brushes.

Similar to the fabrication of homopolymer brushes using PSCAGT, block copolymer brush synthesis requires crystalline diblock copolymers with a tethering point. In this work, we use a triblock copolymer, poly(ethylene oxide)-*b*-poly(L-lactide)-*b*-poly(3-(triethoxysilyl)propyl

methacrylate) (PEO-*b*-PLLA-*b*-PTESPMA), as a model polymer (**Figure 1c**, and see **Figure 2a** for chemical structure). In this polymer, the PLLA block, which serves both single-crystal-templating and brush-forming block functions, is designed for constructing the 2D PSC structure with PEO (brush-forming block) and PTESPMA (tethering block) chains being excluded onto the crystal surfaces. The PEO block is in the solvation state during the PLLA crystallization process and does not affect the PLLA single crystal shape. The PTESPMA segment can serve as the tethering point due to its triethoxysilane pendant groups that can undergo coupling with glass substrates. The reason for introducing such a long coupling block is that if a small coupling end group is used (such as a thiol or a triethoxysilane group), the end group will be shielded by the PEO chains on the PLLA PSC surface (**Figure 1b**). Introducing a long chain bearing surface reactive groups with a comparable volume as the PEO block can facilitate the coupling reaction between the substrate and the single crystal as illustrated in **Figure 1c**.

The triblock copolymer was synthesized by sequential ring-opening polymerization and ATRP starting from PEO monomethyl ether (CH_3O-PEO-OH, M_n = 5,000 g/mol), and the detailed procedure can be found in the Supporting Information. The triblock copolymer has a dispersity (*Đ)* of 1.33 according to the size exclusion chromatography (SEC) data shown in **Figure 2a**. The small tail on the right side of the triblock copolymer's SEC curve is likely due to the uninitiated homopolymer/diblock copolymer chains, which is not uncommon in the block copolymer synthesis. The clear shift of the SEC peak after each polymerization step indicates the formation of the triblock copolymer. The ^{1}H NMR spectrum in **Figure 2b** further confirms the successful synthesis of the polymer, with characteristic signals from PEO, PLLA, and PTESPMA. The total molar mass was calculated based on the PEO initiator and was found to be M_n = 18200 g/mol, with M_n (PLLA) = 8,300 g/mol and M_n (PTESPMA) = 4,900 g/mol. The triblock polymer was also

characterized using differential scanning calorimetry (DSC) with a scanning rate of 10 °C/min. The second heating thermogram shown in **Figure 2c** reveals two endothermic peaks at 47 °C and 138 °C, which are attributed to the melting of PEO and PLLA crystals, respectively. The SEC, ^{1}H NMR, and DSC results confirm the formation of the semicrystalline block copolymer, and therefore it is used for our PSCAGT study.

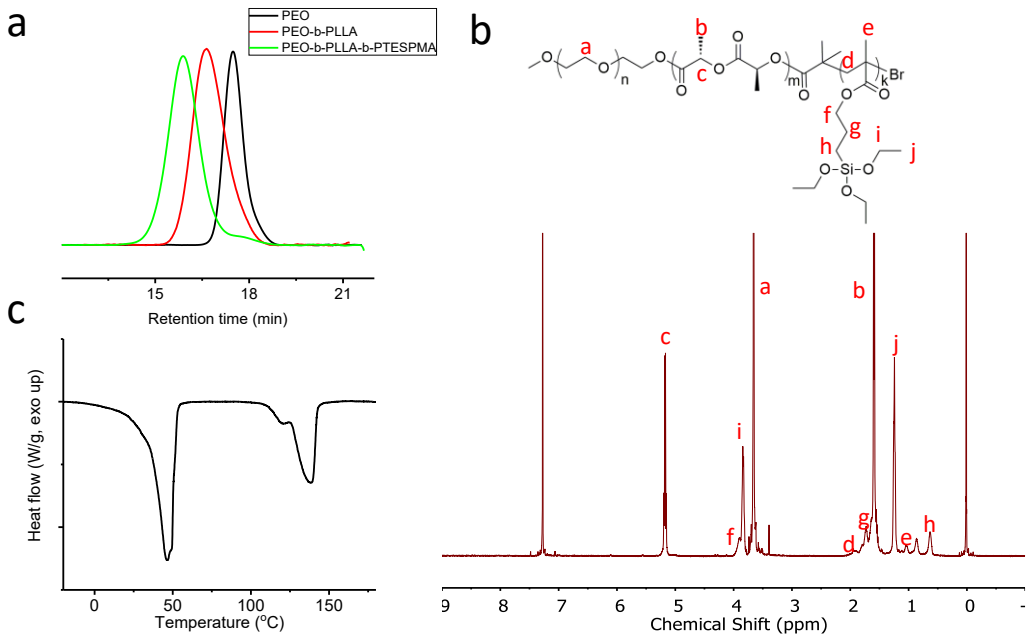

Figure 2. Characterization of triblock copolymer PEO-*b*-PLLA-*b*-PTESPMA. a) SEC curves of PEO, PEO-*b*-PLLA, and PEO-*b*-PLLA-*b*-PTESPMA. b) Chemical structure and ^{1}H NMR spectrum of PEO-*b*-PLLA-*b*-PTESPMA in $CDCl_3$. c) DSC second heating thermogram of the triblock copolymer obtained with a heating rate of 10°C/min.

The synthesis of diblock copolymer brushes follows the previously reported PSCAGT method.[18a] Briefly speaking, the triblock copolymer single crystals were obtained by dissolving the polymer in toluene at 60 °C with a concentration of 0.03 wt.%, followed by slow cooling to

room temperature at a cooling rate of 1 °C/min and crystallization overnight. The crystals were then spin-coated on glass slides freshly activated by a piranha solution, and the coupling reaction was accomplished within 2 h under an ammonia environment. The samples were then washed with chloroform under gentle sonication to remove the untethered polymer chains, leaving only the diblock copolymer brushes on the substrate. The brushes were stored in vacuum at an elevated temperature overnight for further characterization.

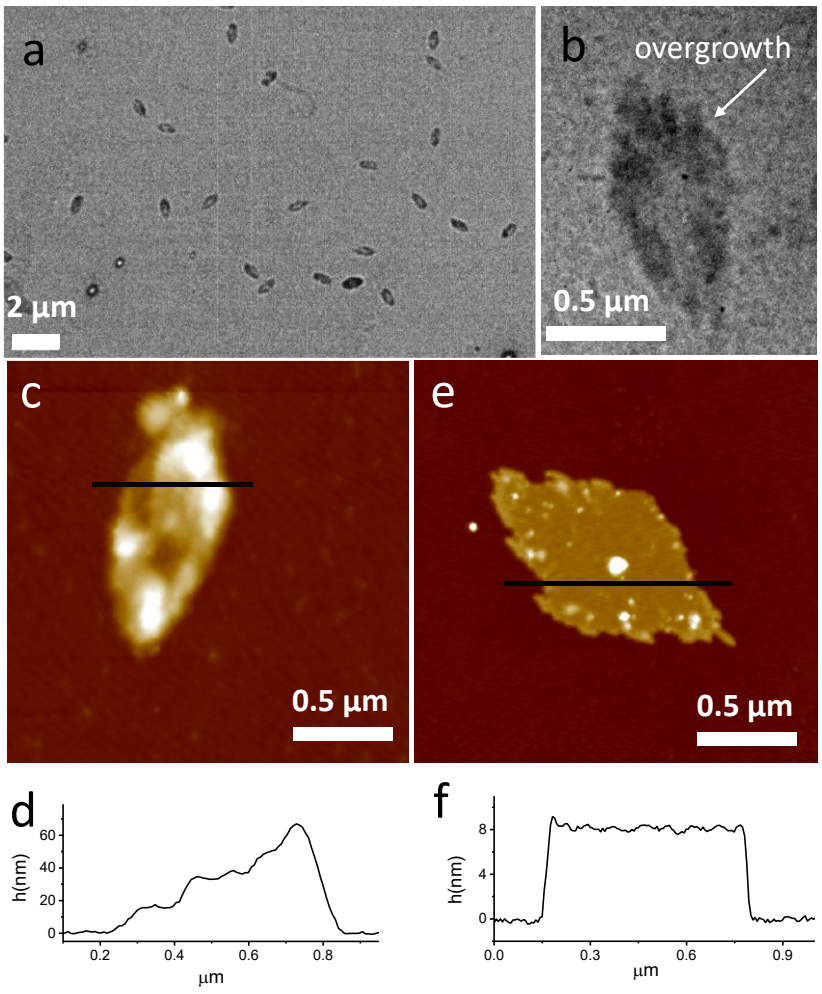

Figure 3. Morphology of the triblock copolymer single crystals and the corresponding diblock brushes. a, b) TEM images of the PSCs of the triblock copolymer under different magnifications. c, d) AFM image and height profile of the PSC spin-coated on a glass slide. e, f) AFM image and height profile of the diblock copolymer brushes on the glass.

Figure 3a shows the TEM image of the single crystals of the triblock copolymer. The crystals all show a lozenge shape, which is consistent with the PLLA single crystal morphology formed in toluene. [20] The histograms of the crystal sizes are shown in **Figure S3**. The lozenge crystals have an average long axis of 0.97 ± 0.03 μm and a short axis of 0.47 ± 0.02 μm, with an aspect ratio of 2.1 ± 0.1, indicating a good control over the uniformity of the size and shape of the crystals. It also appears that the center of the crystals is lighter in contrast. An enlarged TEM image (**Figure 3b**) indicates that there is significant overgrowth around the edge of the crystals, which accounts for the different contrasts in the center and edge regions of the crystals observed in Figure 3a. AFM (**Figure 3c**) also confirms the single crystal morphology and the height profile shows that the single crystal has a thickness of 15.9 ± 0.4 nm (**Figure 3c,d**, and the histogram in **Figure S4a**). Note that the single crystal surface appears rough, which again is due to the overgrowth of the crystal as indicated from the AFM height profile in **Figure 3d**. The 30 nm thickness is twice as the thickness of a single layer, which can be regarded as one layer of overgrowth on the single crystal. The dense overgrowth in the triblock PSCs is likely due to the surface PEO and PTESPMA brushes facilitating the nucleation of a new layer of crystals on the parent lamellar surface.[13b, 21] **Figure 3e** shows the AFM image of the diblock copolymer brushes. The brushes exhibit a lozenge shape similar to that of the single crystal while the brush surface is flat and uniform; no residual overgrown crystals are observed on the block copolymer brushes. The height analysis (**Figure 3f**, and the histogram in **Figure S4b**) shows that the brush thickness is 8.1 ± 0.2 nm, which is approximately half of the polymer single crystal thickness. This is likely due to the evenly distributed tethering blocks on the opposite sides of the single crystal surface, which also suggests a high coupling efficiency of PTESPMA onto glass surface (1.02 ± 0.04 grafting efficiency, where the grafting efficiency is defined as the ratio of total grafted chains and the chains with the

PTESPMA block facing the glass substrate in a PSC. See later discussion). The highly efficient coupling reaction can be attributed to the abundance of triethoxysilane groups in each triblock copolymer chain.

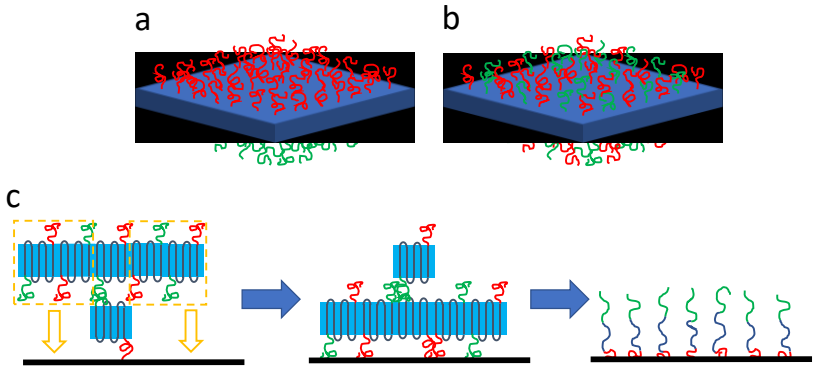

Figure 4. Schematics of the triblock copolymer single crystal with the PEO and PTESPMA blocks a) separated and b) mixed in the crystal. c) Illustration of how uniform polymer brushes are formed from polymer single crystals with surface overgrowth.

As the middle segment of a triblock copolymer crystallizes into a 2D lamellar crystal, the two end blocks can adopt two possible structures: 1) the two end blocks are completely separated and occupy the opposite crystal surfaces (**Figure 4a**); 2) the two end blocks are distributed on both crystal surfaces (**Figure 4b**). Note that only the red blocks can chemically couple onto the flat surface. In case 1, PSCs with the PTESPMA surface facing the glass produce block copolymer brushes with the grafting density identical to that of the PSC, and the resultant brushes thickness therefore should be about the same as that of the PSC. In case 2, uniform block copolymer brushes should be observed with the brush thickness half of the PSC. In the present case, uniform block copolymer brushes are observed with half of the single crystal height (8.1 nm vs. 16 nm), suggesting the triblock copolymer is symmetric (case 2). Note that the overgrowth on the single

crystal does not affect the brush morphology. This can be schematically explained in **Figure 4c**. For overgrown crystal regions, although the crystal thicknesses are different, the chemical structures are the same. As they deposit on the glass substrate, the single-layer region slides onto the glass surface while the overgrown section directly reacts with the substrate, leading to a uniform brush layer.[18a]

One important parameter for polymer brushes is grafting density, which highly affects their properties. In the PSCAGT method, the grafting density is dependent on the crystal structure and can be estimated using the single crystal stem thickness. Here, the PLLA single crystal is sandwiched by PEO and PTESPMA segments, and the thickness d_{PLLA} can be estimated based on the following equation[22]:

$$d_{PLLA} = d_{total} \frac{M_n^{PLLA}/\rho_{PLLA}}{M_n^{PLLA}/\rho_{PLLA} + M_n^{PEO}/\rho_{PEO} + M_n^{PTESPMA}/\rho_{PTESPMA}} \quad (1)$$

where d_{total} is the overall thickness of the PSC; M_n^{PLLA}, M_n^{PEO} and $M_n^{PTESPMA}$ are the molar masses of corresponding blocks; ρ_{PLLA}, ρ_{PEO} and $\rho_{PTESPMA}$ are the densities of the corresponding polymers. Crystalline PEO has a density of 1.239 g/cm^3 while amorphous PEO has a density of 1.124 g/cm^3 [22]. Due to the semicrystalline nature, the overall PEO density is 1.182 g/cm^3 assuming a 50% crystallinity based on DSC results.[22] The density of PLLA is 1.28 g/cm^3, which is not affected by the crystallinity because crystalline and amorphous PLLA have very similar density values.[22] The density of PTESPMA is measured to be 1.08 g/cm^3. Based on equation (1), the PLLA crystal layer in the PSC has a thickness of6.6 ± 0.2 nm. PLLA chain folding number can thus be calculated based on equation (2)[18b] together with PLLA crystal unit cell parameters:

$$\zeta = \frac{\frac{DP_{PLLA}}{n} \times c}{d_{PLLA}} - 1 \quad (2)$$

where ζ is the chain folding number, DP_{PLLA} is the degree of polymerization of PLLA, n is the number of repeating units per chain in one unit cell and c is the c axis unit cell dimension. Here, since the α form PLLA crystal has an orthorhombic unit cell with $a = 1.068\,nm, b = 0.61\,nm, c = 2.886\,nm$ and 10_3 helix conformation[23], the PLLA chain is found to possess a folding number of 4.0. The PLLA crystalline stem areal density $\sigma_{crystal}$ then can be calculated as

$$\sigma_{crystal} = \frac{2}{a \times b} \tag{3}$$

Considering that the PTESPMA segment evenly distributed on the opposite sides of the PSC crystal, we can calculate the diblock copolymer brush grafting density σ_{cal}:

$$\sigma_{cal} = \sigma_{crystal} \times \left\{\frac{1}{(\zeta + 1)} \times \xi\right\} = \frac{2}{a \times b} \times \left\{\frac{1}{(\zeta + 1)} \times \xi\right\} \tag{4}$$

Here ξ denotes the number percentage of PTESPMA segments that are facing toward the surface in a triblock copolymer single crystal (**Figure 4**). In the case of uniform mixing, ξ is 0.5. Taking together, we have σ_{cal} of ~ 0.31 nm^{-2}.

Finally, the polymer brush grafting density can also be estimated based on the AFM brush thickness measurement following the equation:

$$\sigma_{exp} = \frac{\rho h N_A}{M_n} \tag{5}$$

Where ρ is the density of the overall polymer, h is brush thickness and M_n is the total molar mass. The triblock copolymer has an M_n = 18,200 g/mol. After chemical coupling, M_n slightly decreases due to the loss of ethoxy groups. Taking the mass loss into consideration and using an adjusted M_n of 16,200 g/mol, σ_{exp} can be estimated to be 0.36 ± 0.1 nm^{-2}, slightly greater than the calculated σ_{cal}. The difference can be attributed to the possible overestimated brush thickness due

to the extra free volume in the brush region introduced during the crosslinking and chemical coupling reaction, as well as the change of the polymer density during the reaction.

In conclusion, we demonstrated the synthesis of PEO-*b*-PLLA diblock copolymer brushes through a new PSCAGT method. Triblock copolymer PEO-*b*-PLLA-*b*-PTESPMA was designed for this strategy, with PLLA as the crystalline block to grow single crystals and bulky PTESPMA as the coupling block to achieve a high coupling efficiency. The triblock copolymer was synthesized by sequential ring-opening polymerization and ATRP. The crystalline nature of the PLLA and PEO blocks was confirmed using DSC. Solution crystallization was utilized to obtain triblock single crystals with the PLLA blocks being crystallized into lozenge-shaped lamellae and the PEO and PTESPMA blocks on the crystal surfaces. Chemically coupling the PTESPMA to the glass surface leads to the formation of diblock PEO-*b*-PLLA brushes with the PTESPMA blocks forming a crosslinked layer underneath the brush. The polymer brush grafting density was measured to be 0.36 ± 0.1 nm^{-2}, consistent with the calculated value from the PLLA crystalline lattice. While the present study used a 2D flat surface, we anticipate that polymer brushes on curved and/or patterned surfaces with low dimensions can also be prepared using our approach. We envisage this PSCAGT method to be an efficient way to synthesize block copolymer brushes with spatially controlled tethering points and pre-designed single crystal patterns.

Supporting Information

Supporting Information is available from the Wiley Online Library or the authors.

Acknowledgments

This work was supported by the National Science Foundation Grant CHE-1709119 (CYL) and CHE-1709663 (BZ).

References

[1] a) S. T. Milner, *Science* **1991**, 251, 905; b) W.-L. Chen, R. Cordero, H. Tran, C. K. Ober, *Macromolecules* **2017**, 50, 4089; c) A. J. Chancellor, B. T. Seymour, B. Zhao, *Anal. Chem.* **2019**, 91, 6391.

[2] a) J. O. Zoppe, N. C. Ataman, P. Mocny, J. Wang, J. Moraes, H. A. Klok, *Chem. Rev.* **2017**, 117, 1105; b) B. Li, B. Yu, Q. Ye, F. Zhou, *Acc. Chem. Res.* **2015**, 48, 229; c) R. Barbey, L. Lavanant, D. Paripovic, N. Schuwer, C. Sugnaux, S. Tugulu, H. A. Klok, *Chem. Rev.* **2009**, 109, 5437.

[3] M. A. C. Stuart, W. T. S. Huck, J. Genzer, M. Muller, C. Ober, M. Stamm, G. B. Sukhorukov, I. Szleifer, V. V. Tsukruk, M. Urban, F. Winnik, S. Zauscher, I. Luzinov, S. Minko, *Nat. Mater.* **2010**, 9, 101.

[4] a) Y. H. Yin, P. C. Sun, B. H. Li, T. H. Chen, Q. H. Jin, D. T. Ding, A. C. Shi, *Macromolecules* **2007**, 40, 5161; b) G. Brown, A. Chakrabarti, J. F. Marko, *Macromolecules* **1995**, 28, 7817; c) E. B. Zhulina, C. Singh, A. C. Balazs, *Macromolecules* **1996**, 29, 8254; d) E. B. Zhulina, C. Singh, A. C. Balazs, *Macromolecules* **1996**, 29, 6338; e) B. Zhao, W. J. Brittain, W. S. Zhou, S. Z. D. Cheng, *Macromolecules* **2000**, 33, 8821; f) B. Zhao, W. J. Brittain, W. S. Zhou, S. Z. D. Cheng, *J. Am. Chem. Soc.* **2000**, 122, 2407; g) J. Wang, M. Muller, *Macromolecules* **2009**, 42, 2251; h) J. Mandal, A. Arcifa, N. D. Spencer, *Polym. Chem.* **2020**; i) B. M. O'Driscoll, G. H. Griffiths, M. W. Matsen, I. W. Hamley, *Macromolecules* **2011**, 44, 8527; j) O. Guskova, C. Seidel, *Macromolecules* **2011**, 44, 671; k) D. Meng, Q. Wang, *J. Chem. Phys.* **2009**, 130, 134904.

[5] M. A. Rowe, B. A. G. Hammer, S. G. Boyes, *Macromolecules* **2008**, 41, 4147.

[6] S. Kumar, Y. L. Dory, M. Lepage, Y. Zhao, *Macromolecules* **2011**, 44, 7385.

[7] L. Andruzzi, A. Hexemer, X. F. Li, C. K. Ober, E. J. Kramer, G. Galli, E. Chiellini, D. A. Fischer, *Langmuir* **2004**, 20, 10498.

[8] Y. C. Chen, R. Xie, L. Y. Chu, *J. Membr. Sci.* **2013**, 442, 206.

[9] X. M. Zhu, L. Q. Wang, J. P. Lin, L. S. Zhang, *ACS Nano* **2010**, 4, 4979.

[10] R. Poręba, A. de los Santos Pereira, R. Pola, S. Jiang, O. Pop-Georgievski, Z. Sedláková, H. Schönherr, *Macromol. Biosci.* **2020**, 20, 1900354.

[11] Y. F. Hou, J. Q. Jiang, K. Li, Y. W. Zhang, J. D. Liu, *J. Phys. Chem. B* **2014**, 118, 1962.

[12] a) K. Matyjaszewski, P. J. Miller, N. Shukla, B. Immaraporn, A. Gelman, B. B. Luokala, T. M. Siclovan, G. Kickelbick, T. Vallant, H. Hoffmann, T. Pakula, *Macromolecules* **1999**, 32, 8716; b) M. Husseman, E. E. Malmstrom, M. McNamara, M. Mate, D. Mecerreyes, D. G. Benoit, J. L. Hedrick, P. Mansky, E. Huang, T. P. Russell, C. J. Hawker, *Macromolecules* **1999**, 32, 1424; c) K. Matyjaszewski, H. C. Dong, W. Jakubowski, J. Pietrasik, A. Kusumo, *Langmuir* **2007**, 23, 4528; d) B. Zhao, W. J. Brittain, *Macromolecules* **2000**, 33, 8813; e) M. R. Tomlinson, J. Genzer, *Langmuir* **2005**, 21, 11552; f) C. Xu, T. Wu, C. M. Drain, J. D. Batteas, M. J. Fasolka, K. L. Beers, *Macromolecules* **2006**, 39, 3359; g) R. A. Wright, D. M. Henn, B. Zhao, *J. Phys. Chem. B* **2016**, 120, 8036; h) S. N. Ramakrishna, M. Cirelli, E. S. Kooij, M. Klein Gunnewiek, E.

M. Benetti, *Macromolecules* **2015**, 48, 7106; i) D. Hafner, R. Jordan, *Polym. Chem.* **2020**, 11, 2129.

[13] a) P. Geil, *Polymer Single Crystals*, Robert Krieger Pub., Huntington, N. Y. **1973**; b) G. Reiter, *Chem. Soc. Rev.* **2014**, 43, 2055; c) B. Lotz, T. Miyoshi, S. Z. Cheng, *Macromolecules* **2017**, 50, 5995; d) C. Y. Li, *J. Poly. Sci. Poly. Phys.* **2009**, 47, 2436; e) S. Mei, M. Staub, C. Y. Li, *Chem. Eur. J.* **2020**, 26, 349.

[14] a) J. Cai, C. Li, N. Kong, Y. Lu, G. Lin, X. Wang, Y. Yao, I. Manners, H. Qiu, *Science* **2019**, 366, 1095; b) H. Qiu, Y. Gao, C. E. Boott, O. E. Gould, R. L. Harniman, M. J. Miles, S. E. Webb, M. A. Winnik, I. Manners, *Science* **2016**, 352, 697; c) M. Inam, G. Cambridge, A. Pitto-Barry, Z. P. L. Laker, N. R. Wilson, R. T. Mathers, A. P. Dove, R. K. O'Reilly, *Chem. Sci.* **2017**, 8, 4223; d) Y. He, J. C. Eloi, R. L. Harniman, R. M. Richardson, G. R. Whittell, R. T. Mathers, A. P. Dove, R. K. O'Reilly, I. Manners, *J. Am. Chem. Soc.* **2019**, 141, 19088; e) W. Wang, H. Qi, T. Zhou, S. Mei, L. Han, T. Higuchi, H. Jinnai, C. Y. Li, *Nat. Commun.* **2016**, 7, 10599.

[15] a) B. Li, C. Y. Li, *J. Am. Chem. Soc.* **2007**, 129, 12; b) B. B. Wang, B. Li, B. Zhao, C. Y. Li, *J. Am. Chem. Soc.* **2008**, 130, 11594; c) B. B. Wang, B. Li, R. C. M. Ferrier, C. Y. Li, *Macromol. Rapid Commun.* **2010**, 31, 169; d) S. Mei, H. Qi, T. Zhou, C. Y. Li, *Angew. Chem. Int. Ed.* **2017**, 56, 13645; e) B. B. Wang, B. Li, B. Dong, B. Zhao, C. Y. Li, *Macromolecules* **2010**, 43, 9234.

[16] a) S. Cheng, D. M. Smith, C. Y. Li, *Macromolecules* **2014**, 47, 3978; b) S. Cheng, D. M. Smith, Q. Pan, S. Wang, C. Y. Li, *RSC Adv.* **2015**, 5, 48793.

[17] H. Qi, H. Zhou, Q. Y. Tang, J. Y. Lee, Z. Y. Fan, S. Kim, M. C. Staub, T. Zhou, S. Mei, L. Han, D. J. Pochan, H. Cheng, W. B. Hu, C. Y. Li, *Nat. Commun.* **2018**, 9, 3005.

[18] a) T. Zhou, H. Qi, L. Han, D. Barbash, C. Y. Li, *Nat. Commun.* **2016**, 7, 11119; b) S. Mei, C. Y. Li, *Angew. Chem. Int. Ed.* **2018**, 57, 15758; c) T. Zhou, B. Han, H. Qi, Q. Pan, D. M. Smith, L. Han, C. Y. Li, *Nanoscale* **2018**, 10, 18269.

[19] a) W. Y. Chen, J. X. Zheng, S. Z. D. Cheng, C. Y. Li, P. Huang, L. Zhu, H. M. Xiong, Q. Ge, Y. Guo, R. P. Quirk, B. Lotz, L. F. Deng, C. Wu, E. L. Thomas, *Phys. Rev. Lett.* **2004**, 93, 028301 1; b) B. Lotz, A. Kovacs, G. Bassett, A. Keller, *Kolloid-Zeitschrift und Zeitschrift für Polymere* **1966**, 209, 115.

[20] T. Miyata, T. Masuko, *Polymer* **1997**, 38, 4003.

[21] a) M. C. Staub, C. Y. Li, *Polymer* **2020**, 122407; b) H. Qi, W. Wang, C. Y. Li, *ACS Macro. Lett.* **2014**, 3, 675.

[22] J. X. Zheng, H. M. Xiong, W. Y. Chen, K. M. Lee, R. M. Van Horn, R. P. Quirk, B. Lotz, E. L. Thomas, A. C. Shi, S. Z. D. Cheng, *Macromolecules* **2006**, 39, 641.

[23] K. Wasanasuk, K. Tashiro, M. Hanesaka, T. Ohhara, K. Kurihara, R. Kuroki, T. Tamada, T. Ozeki, T. Kanamoto, *Macromolecules* **2011**, 44, 6441.

Supporting Information

Fabrication of 2D Block Copolymer Brushes via a Polymer-Single-Crystal-Assisted-Grafting-to Method

Shan Mei,[1] Jeffrey T. Wilk,[1] Andrew J. Chancellor,[2] Bin Zhao,[2,] and Christopher Y. Li[1,*]*

[1]Dr. Shan Mei, Jeffrey T. Wilk, Prof. Christopher Li, Department of Materials Science and Engineering, Drexel University, Philadelphia, Pennsylvania 19104, United States

[2]Andrew J. Chancellor, Prof. Bin Zhao, Department of Chemistry, University of Tennessee, Knoxville, Tennessee 37996, United States

* Correspondence to: chrisli@drexel.edu; bzhao@utk.edu

Materials

The following chemicals were used as received unless otherwise stated: poly(ethylene oxide) monomethyl ether (MeO-PEO-OH, M_n=5000 g/mol, Polymer Source Inc.), L-lactide (98%, Aldrich), 3-(triethoxysilyl)propyl methacrylate (98%, TCI), 3,5-bis(trifluoromethyl)phenyl isothiocyanate (98%, Aldrich), cyclohexylamine (98%, Aldrich), (−)-sparteine (98%, TCI), 2-bromoisobutyryl bromide (98%, Aldrich), triethylamine (99%, Aldrich), copper(I) bromide (CuBr, 98%, Aldrich), *N,N,N′,N″,N″*-pentamethyldiethylenetriamine (PMDETA, 99%, Aldrich), dichloromethane (99%, anhydrous, Aldrich), chloroform (99%, anhydrous, Aldrich), tetrahydrofuran (99%, anhydrous, Aldrich), toluene (99%, anhydrous, Aldrich), isopropanol (98%, BDH), hexane (95%, anhydrous, Aldrich). L-Lactide was purified by re-precipitation in toluene. 3-(Triethoxysilyl)propyl methacrylate was purified by running through a basic alumina column to remove inhibitors right before polymerization.

Characterization

^{1}H NMR spectra were recorded on a Varian Mercury 500 MHz NMR spectrometer using $CDCl_3$ as the solvent and tetramethylsilane (TMS) as the internal standard. SEC measurements were conducted using a Waters SEC system with a 1525 binary HPLC pump and a Waters 2414 refractive index detector at 40 °C. THF was used as the solvent and the flow rate was 1.0 mL min^{-}

[1]. TEM experiments were conducted using a JEOL JEM2100 instrument with a LaB6 electron source at an acceleration voltage of 120 kV. Polymer single crystal samples were solution cast on carbon-coated copper grids for TEM observation. DSC data were collected using a TA Q-2000 instrument with a scanning rate of 10 °C min^{-1}. Results from the second heating are presented. The instrument was calibrated using indium as the standards. AFM experiments were conducted on a Bruker Multimode 8 instrument using tapping mode. NCHV-A silicon probes with a spring constant of k~42 N m^{-1} and resonance frequency of ~ 320 kHz were used. The images were taken with 512×512 pixels and a scan rate of 1.0 Hz. All AFM samples were prepared on glass slides precleaned by Piranha solution (concentrated H_2SO_4: H_2O_2 (30%) = 4:1). AFM experiments were conducted under a relative humidity of ~20% to minimize the influence of damping on the measurement.[1]

Histograms of the crystals/brushes were obtained based on randomly and evenly selected 20 AFM data points of crystal height, 40 AFM data points of brush height, and 18 TEM data points of the crystal sizes. The uncertainties of the mean values were obtained by calculating the standard deviation from the above results.

Synthesis of Triblock Copolymer

Synthesis of thiourea catalyst 1-(3,5-bis(trifluoromethyl)phenyl)-3-cyclohexylthiourea Thiourea catalyst was synthesized following the literature.[2] Briefly, 3,5-bis(trifluoromethyl)phenyl isothiocyanate (5.0 g, 19 mmol) was dissolved in 20 mL THF in a 50 mL round bottom flask with a magnetic stir bar. Then cyclohexylamine (1.85 g, 18.5 mmol) was added dropwise to the solution with stirring. After stirring for 4 h at room temperature, THF was evaporated and the residue was recrystallized from chloroform to give a white powder.

Synthesis of PEO-b-PLLA-OH MeO-PEO-OH (M_n = 5000 g/mol, 300 mg, 0.06 mmol), L-lactide (604 mg, 4.2 mmol), 1-(3,5-bis(trifluoromethyl)phenyl)-3-cyclohexyl-thiourea (155 mg, 0.42 mmol) were added to a Schlenk flask with a magnetic stirrer and the flask was vacuumed for 30 min to remove moisture. Then, 5 mL anhydrous chloroform and (−)-sparteine (49 mg, 0.21 mmol) were added sequentially to the flask. The solution was stirred at 30 °C for 3 h. The polymers were then precipitated in isopropanol, filtered, and dried under vacuum. The ^{1}H NMR and SEC results are shown in Figure S1 and Figure 2a. The peak at δ = 3.7 in the ^{1}H NMR spectrum is from PEO. Peaks at δ = 1.6 and δ = 5.2 are from the PLLA block. Based on the molar mass of PEO macroinitiator (M_n(PEO)=5,000 g/mol), the molar mass of PLLA is M_n(PLLA) = 8,300 g/mol. The dispersity of the block copolymer is $Đ$ = 1.25 according to the SEC data.

Synthesis of PEO-b-PLLA-Br PEO-*b*-PLLA-OH (M_n = 13,300 g/mol, 100 mg, 0.0075 mmol) and triethylamine (7.6 mg, 0.075 mmol) were dissolved in anhydrous dichloromethane in a round bottom flask. 2-Bromoisobutyryl bromide (17.3 mg, 0.075 mmol) was added dropwise to the flask in an ice bath under vigorous stirring. The solution was allowed to react overnight at room temperature. The polymer was precipitated in isopropanol, filtered and dried in vacuum. The polymer was characterized by ^{1}H NMR analysis as shown in Figure S2. In the NMR spectrum, most of the peaks have the same chemical shifts and relative integrals as those in PEO-*b*-PLLA-OH, the only difference is the peak at δ = 1.9 ppm, which is the characteristic peak of -CH_3 at the chain end confirming the successful modification with the ATRP initiator. The conversion of the chain ends was determined to be 98% based on the integration of the peaks.

Synthesis of PEO-b-PLLA-b-PTESPMA The above synthesized PEO-*b*-PLLA-*b*-Br (M_n = 13,300 g/mol, 100 mg, 0.0075 mmol), 3-(triethoxysilyl)propyl methacrylate (96 mg, 0.33 mmol), and *N,N,N′,N″,N″*-pentamethyldiethylenetriamine (PMDETA, 1.3 mg, 0.0075 mmol) were dissolved in 1 mL anhydrous toluene in a Schlenk flask. The solution was degassed through three freeze-pump-thaw cycles to remove oxygen. Then CuBr (1.1 mg, 0.0075 mmol) was added to the flask under nitrogen protection. The solution was stirred at 90 °C for 1 h before being quenched to room temperature. The polymer was precipitated in anhydrous hexane, filtered, and stored under vacuum. The polymer was characterized by ^{1}H NMR and SEC as shown in Figure 2a. ^{1}H NMR spectrum shows all the characteristic peaks from the PTESPMA block as labeled while all the peaks from PEO and PLLA blocks remained unchanged. The molar mass of PTESPMA block was calculated based on the ^{1}H NMR analysis to be M_n (PTESPMA) = 4900 g/mol. The dispersity is $Đ$ = 1.33 according to the SEC data.

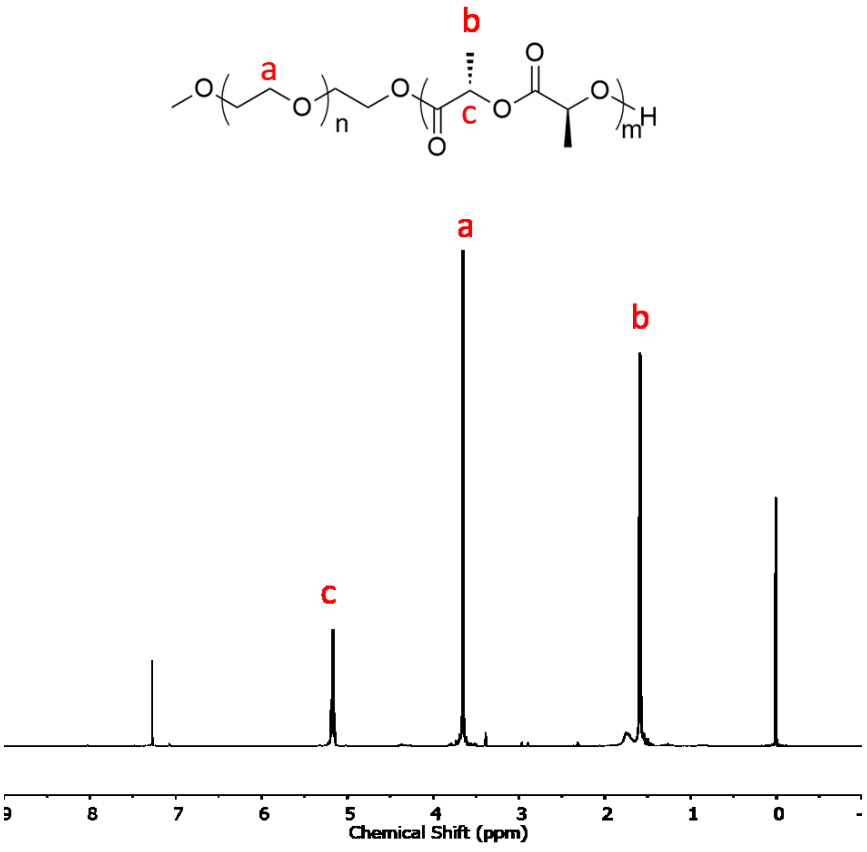

Figure S1. ^{1}H NMR spectrum of PEO-*b*-PLLA-OH in $CDCl_3$.

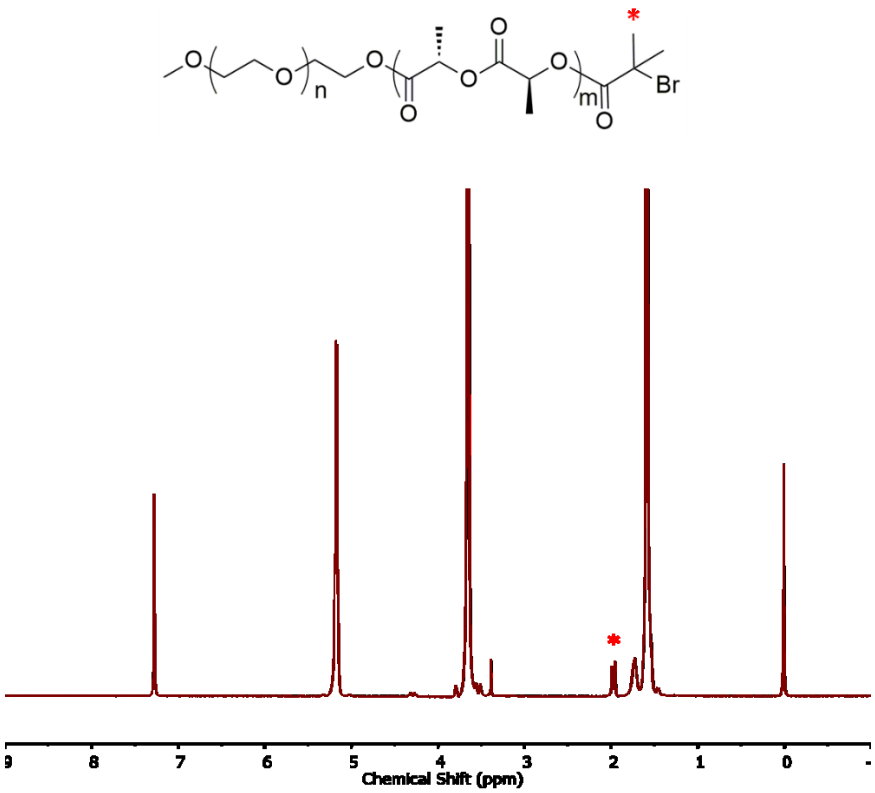

Figure S2. ^{1}HNMR spectrum of PEO-*b*-PLLA-Br in $CDCl_3$.

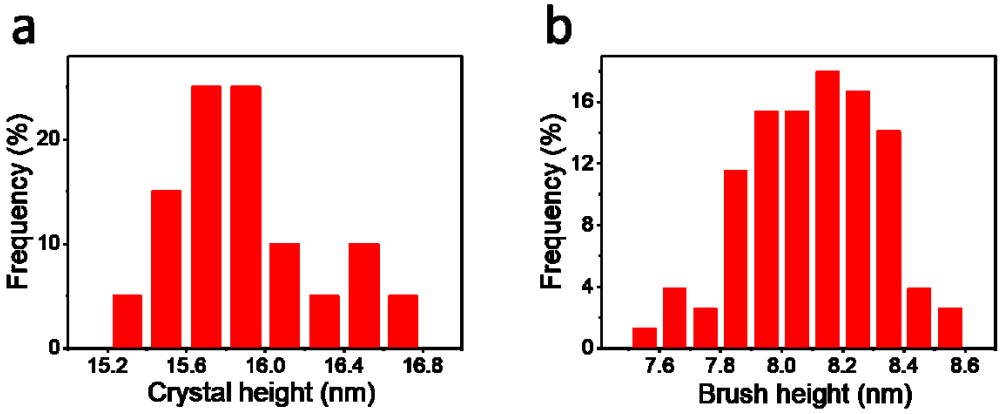

Figure S3. Histograms of the a) triblock copolymer single crystal height and b) diblock copolymer brush height.

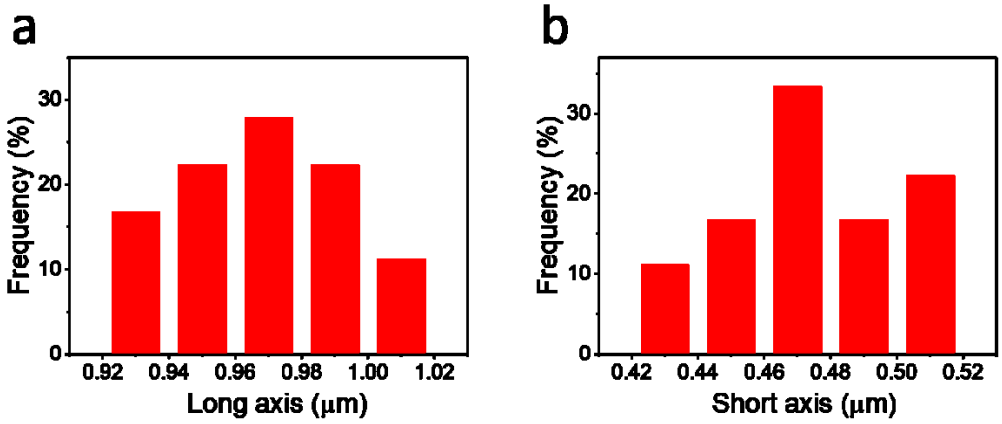

Figure S4. Histograms of triblock copolymer single crystals showing the a) long axis and b) short axis.

Calculation of the density of the triblock copolymer PEO-*b*-PLLA-*b*-PTESPMA after the surface coupling and crosslinking

The density is calculated based on the following equation:

$$\rho = \frac{M_n^{PEO-b-PLLA-b-PTESPMA}}{M_n^{PEO}/\rho_{PEO} + M_n^{PLLA}/\rho_{PLLA} + M_n^{PTESPMA}/\rho_{PTESPMA}}$$

where M_n and ρ are the molar mass and density of corresponding block/polymer, based on the data listed in the main text, the density of the triblock copolymer is ρ = 1.18 g/cm^3.

[1] S. J. van Noort, K. O. van der Werf, B. G. de Grooth, N. F. van Hulst, and J. Greve, *Ultramicroscopy* **1997**, 69, 117-127.

[2] R. C. Pratt, B. G. G. Lohmeijer, D. A. Long, P. N. P. Lundberg, A. P. Dove, H. B. Li, C. G. Wade, R. M. Waymouth, J. L. Hedrick, *Macromolecules* **2006**, 39, 7863-7871.